RSC Advances

ROYAL SOCIETY OF CHEMISTRY

www.rsc.org/advances

Table of contents entry

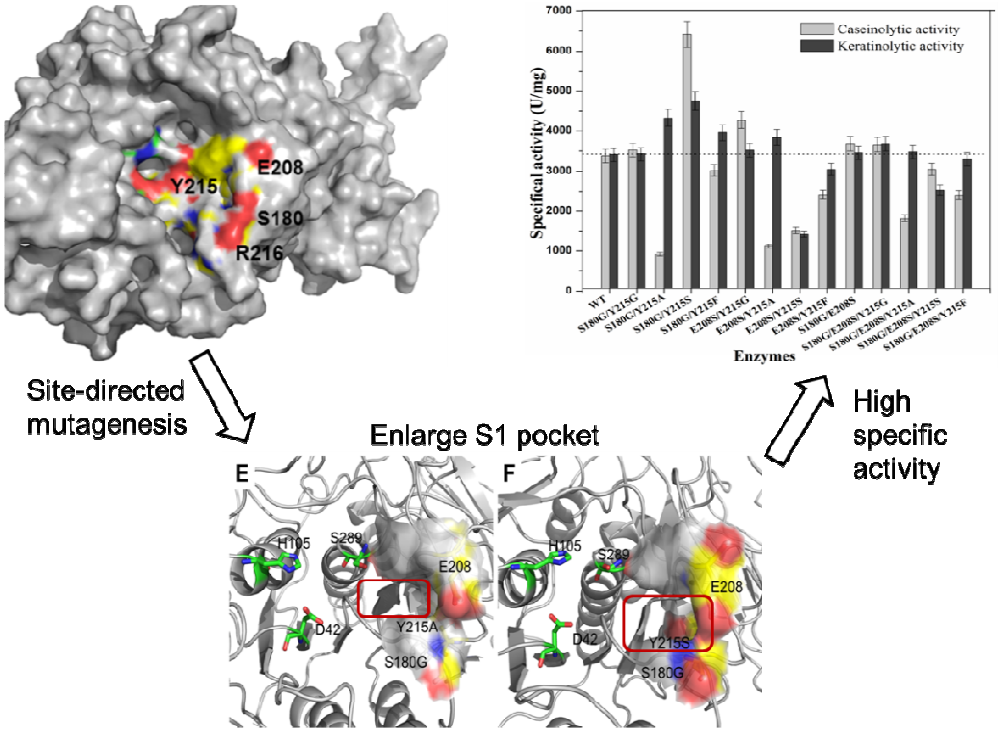

Mutagenesis at position 215 could shift the catalytic ability of keratinase KerSMD to hydrolyze synthetic peptides and macromolecular substrates. We improved keratinolytic activity of five mutants and obtained two thermophilic keratinases.

Insight into the substrate specificity of keratinase KerSMD from *Stenotrophomonas maltophilia* by site-directed mutagenesis studies in S1 pocket

Zhen Fang,[a, b, e] **Juan Zhang,**[a, e,*] **Baihong Liu,**[a, b, e] **Guocheng Du,**[c,e,*] **Jian Chen** [d,e]

[a] *Key Laboratory of Industrial Biotechnology, Ministry of Education, Jiangnan University, Wuxi 214122, China*

[b] *Synergetic Innovation Center of Food Safety and Nutrition, Wuxi 214122, China*

[c] *Key Laboratory of Carbohydrate Chemistry and Biotechnology, Ministry of Education, Jiangnan University, Wuxi 214122, China*

[d] *National Engineering Laboratory for Cereal Fermentation Technology, Jiangnan University, Wuxi 214122, China*

[e] *School of Biotechnology, Jiangnan University, Wuxi 214122, China*

* Corresponding authors

Juan Zhang, E-mail: zhangj@jiangnan.edu.cn, Tel.: +86-510-85918307, Fax: +86-510-85918309.

Guocheng Du, E-mail: gcdu@jiangnan.edu.cn. Tel./Fax: +86-510-85918309.

School of Biotechnology, Jiangnan University, 1800 Lihu Road, Wuxi 214122, China.

Abstract

The keratinase KerSMD from *Stenotrophomonas maltophilia* can hydrolyze broad substrates but its keratinolytic activity needs to be improved for industrial application. From sequence alignment and homologous modeling, we deduced that four residues, Ser180, Glu208, Tyr215, and Arg216, lying at the entrance or bottom of the S1 pocket, were related to the substrate specificity. The S1 pocket was enlarged by mutating a series of amino acids. We found that mutagenesis at position 215 could shift the catalytic ability of KerSMD to hydrolyze synthetic peptides and macromolecular substrates. We improved the keratinolytic activities of five mutants (Y215G, Y215S, Y215A, S180G/Y215A, and S180G/Y215S) and obtained two thermophilic keratinases (Y215S and S180G/Y215S). Compared to the wild type, the S180G/Y215S showed the highest keratinolytic activity (4755 U mg^{-1}) and the S180G/Y215A showed the most excellent specificity to degrade feather. Our results indicate that steric hindrance and hydrophilia in the S1 pocket have a significant effect on feather keratin preference of keratinase, and the hydrogen bonds in S1 pocket have great influence on thermostability. These findings not only give an insight into the relationship between S1 pocket and substrate specificity but also suggest approaches for protein engineering of keratinase.

Keywords: keratinase; site-directed mutagenesis; substrate specificity; S1 pocket; steric hindrance

1 Introduction

Keratinase is a well-known protease used in degrading insoluble keratin substrates, such as feather, wool, hair, and horn, which are not easily digested by common proteases (papain, pepsin, and trypsin) because of the existence of disulfide bonds and highly hydrophobic interactions.[1-5] It has been reported that feather waste can be transformed into feed additives by keratinase.[6] Besides the effective application on feather recycling, keratinase also has great potentials in leather treatment, textile process, peptide production, and fertilizer industry.[7-10]

Nowadays, there is a growing demand of keratinase for the industrial application.[11, 12] Industrial enzymes always need high specific activity, temperature stability, and inoxidizability. Keratinolytic activity or substrate specificity is one of the important biochemical properties to determine whether a novel keratinase has a commercial prospect.[9, 11] However, commercially available keratinases are rare because of their low activities or thermostabilty to degrade keratin substrates.

Improving the specific activity or other characterizations by protein engineering is a fast way to get satisfactory keratinases. Protein engineering, such as site-directed mutagenesis and directed evolution, is the common technique to obtain an excellent enzyme. Nevertheless, the directed evolution by random mutations may need a lot of work to screen an excellent enzyme.[18] Since many keratinases belong to the subtilisin-like protease and they often share highly conserved amino acid sequences, site-directed mutagenesis based on homology modeling can be used to modify enzyme characteristics.[7, 11, 13] For example, a conserved Gly166, located at the bottom

of substrate binding pocket of subtilisin BPN', was substituted to nonionic amino acids to change its specificity to different hydrophobic substrates.[18] So, the site-directed mutagenesis is convenient to shift the substrate specificity by changing the size or electrostatic interactions of the substrate binding cleft.[14-17]

Since keratinase is a new-type enzyme and its mechanism on degrading keratin is unclear, broadening its industrial application by random mutagenesis is difficult. However, changing substrate binding pocket may overcome keratinase disadvantages, such as low keratinolytic activity and low thermostability. There are many substrate binding pockets on protease surface, and the pocket close to three catalytic residues (His, Asp, and Ser) is called S1 pocket, which also exists in keratinase.[28,34] Except for subtilisin BPN', crystal structures and molecular modifications of proteases were investigated and it stated that S1 pocket is important to identify special residues for binding and catalysis.[18] Since the S1 pocket is the main factor affecting substrate specificity of subtilisin protease, it is interesting to investigate whether the S1 pocket of keratinase has the similar function and to explain its catalytic mechanism.

In our previous study, a novel keratinase named KerSMD from *Stenotrophomonas maltophilia* BBE11-1 has been isolated for potential feather digestion and textile treatment.[20, 21] Compared to the commercial keratinase KerA, KerSMD has excellent heat stability and substrate specificity for degrading feathers.[21, 22] However, its keratinolytic activity does not meet the industrialization demands. The catalytic domain of KerSMD shows high identity (48%) with subtilisin-like proteases (Protein Data Bank: 3LPA, 3LPD, 3TI7, and 3TI9), providing its possibility for

homology modeling.[21] In this report, the alignment of amino acid sequences between KerSMD and other keratinolytic subtilisins were conducted to determine the key residues in the S1 pocket. We selected four amino acids (Ser180, Glu208, Tyr215, and Arg216) for site-directed mutagenesis. Enzyme activities towards micromolecular substrates (synthetic peptides) and macromolecular substrates (casein and feather) were assayed. Our results indicate that the change of S1 pocket can affect substrate specificity, thermostability, and keratinolytic activity. The possible function of S1 pocket may provide new clues for protein engineering of keratinase.

2 Experimental

2.1 Bacterial strains, plasmids, and materials

The keratinase KerSMD gene (GenBank accession number KC814180) from *S. maltophilia* BBE11-1 was cloned into plasmid pET-22b according to the previous work.[21] The hosts for plasmid cloning and expression were *Escherichia coli* JM109 and BL21 (DE3), respectively. PrimeSTAR HS DNA polymerase, PCR reagents, and competent cell preparation kit were purchased from TaKaRa (Dalian, China). Plasmid extraction and DNA sequencing were conducted by Sangon (Shanghai, China). Restriction endonucleases were obtained from Fermentas (Shanghai, China). *N*-Succinyl-Ala-Ala-Pro-Ala-*p*-nitroanilide (AAPA), *N*-Succinyl-Ala-Ala-Pro-Val-*p*-nitroanilide (AAPV), *N*-Succinyl-Ala-Ala-Pro-Phe-*p*-nitroanilide (AAPF), and *N*-Succinyl-Ala-Ala-Pro-Leu-*p*-nitroanilide (AAPL) were from Sigma-Aldrich (Saint Louis, USA). Feather meal was prepared from local farm.

Other analytical grade reagents were all purchased from Sangon.

2.2 Media and culture conditions

The Luria-Bertani (LB) medium containing 100 μg ml^{-1} ampicillin was used for the recombinant *E. coli* bacteria to grow. The seed culture was incubated at 37 °C with sufficient shaker (200 rpm). When the bacterial density reached OD_{600} 0.6, isopropyl-*β*-D-1-thiogalactopyranoside (IPTG) was added to the medium of *E. coli* BL21 (DE3) to a final concentration of 0.1 mM. The temperature for fermentation culture was also decreased to 20 °C. After 72 h incubation, the broth was centrifuged to obtain cell-free supernatant.

2.3 Site-directed mutagenesis

With the plasmid kerSMD/pET-22b, we obtained new mutants by one-step PCR method. The site saturation mutagenesis of Tyr215 was carried out with mutagenic primers 5'-ACAACGCTTCCAAGNNKCGTCCGGCCAGTTG-3' (N represents A, T, G, or C, and K represents G or T). The double mutants were constructed using the first PCR mutagenesis as the template. Then, all PCR products were digested with DpnI endonuclease at 37 °C for 1 h. The reaction mixture containing the new mutants was transformed into *E. coli* JM109. The correct mutants were checked by DNA sequencing and then transformed into the expression host of *E. coli* BL21 (DE3).

2.4 Purification of KerSMD and its mutants

The fermentation supernatant of recombinant *E. coli* BL21 (DE3) was collected

and resuspended in 30% (w/v) solid ammonium sulfate solution. The purification method was according to the former reference.[21] The sample was purified by hydrophobic interaction and anion exchange columns with the AKTA pure system (GE Healthcare, Sweden). The keratinolytic fractions were collected and dialyzed against buffer A (20 mM Tris-HCl, pH 8.5) overnight. Then, the enzyme solution was submitted to Q-Sepharose HP (GE Healthcare, Sweden) by using equilibrium buffer A. Buffer B (20 mM Tris-HCl and 1M NaCl, pH 8.5) with a linear gradient from 0% to 100% was used to elute keratinases. The keratinolytic fractions were obtained for sodium dodecyl sulfate polyacrylamide gel electrophoresis (SDS-PAGE) analysis reported by Fang *et al*.[21] The enzyme solution was preserved at -80 °C.

2.5 Caseinolytic and keratinolytic activity assays

The caseinolytic activity was based on the release of tyrosine during the hydrolysis of casein. Enzymes (100 μl) with different concentrations were added to 200 μl buffer C (50 mM Gly-NaOH, pH 9.0) containing 1% (w/v) casein. Then the mixture was incubated at 50 °C for 10 min. The reaction was terminated by the addition of 200 μl 4% (w/v) trichloroacetic acid (TCA), and then centrifuged at 10, 000 × *g* for 10 min. The Folin-Phenol reagent was used to measure the amount of released tyrosine. One unit (U) of caseinolytic activity was defined as per ml enzyme required to release one μmole tyrosine per minute.

Keratinolytic activity was determined at 50 °C for 60 min in a 1 ml reaction mixture including of 50 mg feather meal and different concentration of keratinase in

buffer C. The reaction was stopped by adding the 1 ml 4% (w/v) TCA. After centrifugation at 10, 000 × *g* for 10 min, the OD_{280} of supernatant was measured. The definition of one unit (U) keratinase activity was described as the 0.001AU increase of absorbance at 280 nm.

2.6 Temperature and pH stability of wild type and mutants

The optimal reaction temperature and enzyme thermostability are measured by incubating the purified enzymes at various temperatures (30-80 °C, 20 mM phosphate buffer, pH 7.0). The half-life ($t_{1/2}$) of enzyme activity at 50 °C was determined. The optimal reaction pH of the wild type and mutants were also assayed by maintaining samples at different pHs (pH 5.0 to 12.0). The buffers considered to adjust pH ranges were NaAc-HAc (pH 4.0 to 6.0, 100 mM), Na_2HPO_4- NaH_2PO_4 (pH 6.0 to 8.0, 100 mM), Tris-HCl (pH 8.0 to 9.0, 100 mM), and Glycine-NaOH (pH 9.0 to 12, 100 mM). The highest enzyme activity was considered as 100%, and the relative activities were recorded as a percentage. All assays were performed in triplicate with an experimental error under 5%.

2.7 Kinetic parameters of wild type and mutants

Four synthetic peptides (AAPL, AAPF, AAPV, AAPA) containing different hydrophobic amino acids in P1 site were used to investigate the changes of kinetic parameters. The method was based on Windhorst *et al*.[23] The reaction was conducted in buffer D (100 mM Tris-HCl, 5% v/v dimethylformamide, pH 8.2) at 25 °C. The

enzyme concentration was varied between 9.0×10^{-9} M and 2.0×10^{-8} M, and the substrate was in the range of 0.1 to 1.6 mM. An absorbance at 405 nm (ε_{405} = 9600 M^{-1} cm^{-1}) was measured at 0.1s intervals with UV2450 spectrophotometer (Shimadzu, Japan) to monitor the release of *p*-nitroaniline. The kinetic parameters of K_m and k_{cat} were obtained by nonlinear regression analysis with the software UVProbe. The various substrates were repeated at least two times with a standard deviation under 5%.

2.8 Model constructions of wild type and mutants

In order to determine the constitution of the S1 pocket, the homology models of KerSMD and other mutants were constructed with the program Modeller V9.11.[24] The model of the catalytic domain was based on the crystal structures of subtilisin-like proteases (Protein Data Bank: 3LPA, 3LPC, 3LPD, 3TI9, 3TI7, 1DBI, 1THM, 3AFG) while the PPC domain was constructed with the temples of vEP C-ter 100 (PDB: 2LUW) and kexin (PDB: 1OT5). After the catalytic domain and PPC domain were linked together by the program Discovery Studio V2.5 (Accelrys, San Diego, CA), the model of KerSMD was obtained by choosing the lowest score model and the models of mutants were designed by using the protocol Build Mutants. Molecular dynamics (MD) simulations by NAMD software (http://www.ks.uiuc.edu/) were conducted for energy minimization and fully reducing the steric clashes. The CHARMM force field, periodic boundary condition of water box, and Particle Mesh Ewald (PME) algorithm were employed. By setting a constant temperature of 310 K, 1 atm pressure, and 1 ns

running time, the whole system was fully relaxed to obtain the minimum energy models. The online tools of PROCHECK, ERRAT of SAVES (http://services.mbi.ucla.edu/SAVES/) showed the stereochemical quality value to be 95%.

3 Results and discussion

3.1. Selection of mutagenesis sites

Since KerSMD had a subtilisin-like catalytic domain, the keratinase model was conducted according to similar proteases. [34] As shown in Fig. 1A, the model structure clearly showed that KerSMD had a catalytic triangle (Asp42, H105, and Ser289) and a S1 pocket (Ser176-Ser180, Ala204-Glu208, and Tyr215-Ala218). The residue Tyr215 of KerSMD, located in the chain-binding cleft, has an uncharged polar side chain; while the Arg216 is the strong hydrophilic residue near the bottom of the S1 pocket (Fig. 1B). Comparing the S1 pockets of various keratinolytic proteases (BprV, Fervidolysin, and KerA) and other subtilisins (E and BPN'), we found that pockets mainly consisted of hydrophobic amino acids and shared high homology (Fig. 1C). However, Ser180, Glu208, Tyr215, and Arg216 are high hydrophilic amino acids. Furthermore, the structure model revealed that Glu208 and Tyr215 with long and polar chains were a hidden trouble to block the binding of P1 substrate (Fig. 1). To investigate whether the steric volume or hydrophobicity affected the substrate specificity of keratinase KerSMD, we constructed E208N, E208S, Y215T, Y215Q, Y215G, R216W, and R216Y mutants. The substitution might decrease hydrophilic

and steric hindrance of the S1 pocket and change substrate specificity.

3.2. First round site-directed mutagenesis in S1 pocket

The purified keratinase KerSMD and its mutants (S180G, E208N, E208S, Y215G, Y215T, Y215Q, R216W, and R216Y) were subjected to 10% SDS-PAGE to estimate their molecular sizes which were all about 44 kDa based on a single band on SDS-PAGE (see supplementary Fig. S1). Their biochemical characterizations were assayed and shown in Table 1. Compared with the wild type, the mutants S180G and Y215Q had a lower optimal reaction temperature (55 ^{o}C) and pH (7.0). The optimal temperature of E208S and Y215T increased to 70 ^{o}C and 65 ^{o}C, respectively; while their optimal pH increased to 9.0. It indicated that lower charge side chain might change thermostability and alkaline stability.

Besides, four synthetic peptides, each different at the P1 site, were used to reveal the substrate specificity of the S1 pocket. Table 1 showed that wild type and mutants all preferred to hydrolyze phenylalanine at the P1 site. The Y215G exhibited the highest activity towards AAPF and AAPL while its activity towards AAPV was the lowest. Only the mutant Y215Q decreased activity towards all four synthetic peptides. It seemed that replacing the Tyr215 with short side-chain residues could significantly improve catalytic efficiency to larger P1 residue, such as Phe. Substrate selectivity of R216W and R216Y did not change much. Our results showed that long and hydrophilic side chains in S1 pocket might restrict substrate preference.

The mutagenesis of position Tyr215, i.e., the bottom of the S1 pocket, also

brought out strong effects to catalyze macromolecular substrates. As shown in Table 1, Y215G mutant has the highest protease activity in degrading soluble casein and insoluble feather while the hydrophilic substitution of Y215Q suffered an obvious decrease in the keratinolytic activity. Mutagenesis results in the Tyr215 site showed that keratinolytic activity was probably related to the hydrophobic and short chains. Other reduction of steric hindrance also had a slightly positive effect on the enzyme activity. Asparagine, a strong hydrophilic peptide but small steric hindrance substituted at position 208, promoted all protease activities. Serine is less charged than Asp and Glu, and the mutant E208S had a lower caseinolytic activity, indicating that hydrophobicity at position 208 might be negative. There were on obvious changes to other mutants, such as R216W and R216Y.

3.3. Mutagenesis with nonionic amino acids at Tyr215

Since our first round site-directed mutagenesis showed that keratinolytic activity of keratinase might be related hydrophobic position of Tyr215, we chose some nonionic amino acids for substitution of Tyr215. Highly hydrophilic Y215N and Y215P decreased keratinase activity when compared with the same volume residue of Y215T (Table 2). By increasing the hydrophobicity at Tyr215, it only obtained a few mutants with improved caseinolytic or keratinolytic activity (Table 2). The excellent mutants were Y215S, Y215T, Y215G,Y215A, and Y215F. The side chain volume of Y215S was close to Y215A, but Y215A was more hydrophobic and yielded the better substrate specificity to degrade keratin (Table 2). Glycine, which is a nearly neutral

hydrophobic amino acid and has the smallest steric volume, yielded the maximum caseinolytic and keratinolytic activity. It indicated that hydrophobicity was not the most important fact to affect enzymatic activities. In fact, the volume of side chains had important effect on keratinolytic activity. For example, the similarly hydrophobic mutants Y215A and Y215M showed obvious difference in keratinolytic activity. Because of the smaller volume of Ala at Tyr215, it contributed to a larger S1 pocket and higher keratinolytic activity. The heavy side chain of Y215W also resulted in tremendous decrease of keratinolytic activities. So the bulkiness of the side chains may have more weight than hydrophobicity on enzymatic activities.

The space volume of side chain of Tyr215 has great effect on catalytic kinetics of S1 pocket. The residue at position 215 was mutated into uncharged polar or nonpolar side chains and analyzed kinetically with an increasing size in the side chains.[25] The mutant Y215N was the highest hydrophilic side chain and considered as the control according to Kyte *et al*.[26] As shown in Fig. 2, the change in position 215 resulted in different P1 substrate specificity. With the increase in the side chain volume, the catalytic efficiency of the mutants (from Gly215 through Cys215) showed decreasing tendency for the substrate AAPF and AAPL. Although Cys and Thr are similar steric chains, the different decreasing curve appeared between Cys215 and Thr215. It was deduced that Cys was more hydrophilic and was oxidized more easily. Upon further increasing the side chain volume from Pro to Trp, there were no further decrease in k_{cat}/K_m value, and AAPF remained the preferred substrate. The catalytic efficiency to AAPA substrate was the highest for Phe215 (Fig. 2). Although the volume of Tyr215

and Phe215 are similar, the Tyr215 with hydrophilic side chain showed obvious decrease of k_{cat}/K_m value to AAPA. The same case was also happened to the Met215, which shared similar side chain volume of 102 $Å^3$ to Ile215 and Leu215 but suffered serious decline of catalytic efficiency. However, not all mutants with large side chains could inhibit keratinolytic activity. For example, the large steric hindrance of mutant Y215F showed similar activity to Y215T, indicating that Phe215 probably formed intermolecular forces with keratin substrate.

3.4. Combinational mutations at position S180, E208 and Y215

In order to further verify the importance of the S1 pocket, we constructed the different combinational mutants at position S180, E208 and Y215, and their enzymatic properties were characterized. After the introduction of short and hydrophobic side chains in the S1 pocket, the catalytic efficiencies were improved towards AAPF (Table 3). The S180G/Y215S obtained the maximum k_{cat}/K_m value. On the other hand, the introduction of hydrophilic residues resulted in about 50% decrease in the activities of E208S/Y215S and S180G/E208S/Y215S to catalyze AAPF. Those two mutants also showed a decrease in keratinolytic activity and E208S/Y215S showed the lowest value. We deduce that excessive hydrophilicity of the S1 pocket might inhibit catalytic activity to AAPF and feather keratin. In addition, we observed that K_m value was greatly lowered by the triple mutation S180G/E208S/Y215G which consisted of substitution with small amino acids in the S1 pocket. We deduced that S1 pocket consisting of three flexible substitutions was

against its binding ability and activity. Combinational mutations that involved position Glu208 might be negative (Fig. 3). It had reported that Glu could form hydrogen bonds with other residues.[27] So it probably resulted from the loss of hydrogen bonds to maintain the structure stability of the S1 pocket.

The protease activities of combinational mutants on casein and feather also showed different results. The polar and nonpolar side chains at position 215 showed tremendous differences in hydrolyzing casein substrate. In detail, S180G/Y215A and E208S/Y215A yielded the highest substrate specificity to feather but their activities on casein were the lowest (Fig. 3). Contrarily, the substitution of Ser in the position Tyr215 yielded both the highest activities of S180G/Y215S on casein and feather (Fig. 3). Replacing Phe in position 215 showed a little effect on protease activities of S180G/Y215F.We also observed that four mutants, E208S/Y215S, E208S/Y215F, S180G/E208S/Y215S, and S180G/E208S/Y215F, decreased activities on both casein and feather, and the activity value of E208S/Y215S is the lowest (Fig. 3). It indicated that hydrophilic substitution has negative effect on S1 pocket and decreases protease activities.

3.5. Temperature effect on five high-activity mutants

Since site-directed mutagenesis in S1 pocket has great effect on spatial structure and may change protein stability, it is important to investigate the optimal reaction temperature and thermostability of mutants. In total, five mutants, Y215G, Y215S, Y215A, S180G/Y215A, and S180G/Y215S, obtained higher keratinolytic activities

318 and were considered for further analysis. The 50 °C was chose for thermostability
319 analysis because temperatures between 40 °C and 60 °C were the best conduction for
320 feather degradation treatment and showed lowest damage to amino acids.[1] Fig. 4A
321 showed that three mutants, Y215G, Y215S, and S180G/Y215S, shifted their optimal
322 reaction temperature from 50 °C to 60 °C. And Y215S mutant achieved the maximum
323 keratinolytic activity (nearly 7000 U mg^{-1}) at 60 °C, more than 2-fold of that wild
324 type. Keratinases with improved thermophilic property can be used in food processing
325 or feed additives which always need short-time sterilization at high temperature.[4] Fig.
326 4B showed that Y215S mutant had high thermostability, indicating its great potential
327 in feather waste treatment at 50 °C. However, introducing of Gly at position 180 or
328 215, Y215G, S180G/Y215A, and S180G/Y215S decreased their highest keratinolytic
329 activities at 40 °C, approaching the temperature of poultry and promoting feather
330 digestion in stomach and intestines. Y215A and S180G/Y215A showed a decrease in
331 heat stability (Fig. 4B). It is known that glycine and alanine are flexible and may
332 change enzyme structure, and the hydrophobic alanine on the protein surface may
333 reduce enzyme stability in an aqueous solution.

334 **3.6. Structure modeling and analysis of wild type keratinase and mutants**

335 Structure modeling and analysis of the wild type and mutants (Y215A, Y215S,
336 Y215G, S180G/Y215A, and S180G/Y215S) were studied in Fig. 5, which showed
337 that constitutive factors of substrate-binding clefts were important to keratinolytic
338 activity of KerSMD. The substitutions of Gly and Ser were all short side chains,

opening the pocket entrance to bind to a larger residue at the P1 site (Fig. 5). We deduce that the size of the S1 pocket is the main factor on substrate selectivity. This was proved by mutagenesis in the S1 pocket which had a significant effect on the keratinolytic activity and the P1 specificity to synthetic substrates. Since Phe at the P1 position of AAPF shows obvious steric hindrance and high hydrophobicity, the size of the S1 pocket needs to be sufficiently larger to bind a substrate. The hydrophobic pocket also contributes its high binding ability to hydrolyze AAPF or AAPL.[16, 28] It has been reported that the S1 pocket of subtilisin-like protease is near the catalytic center and binds to special residues in the protein substrate.[28-30] KerSMD has a subtilisin-like catalytic domain and broad specificity to hydrolyze casein, collagen, and keratin, and it may be related to the S1 pocket.[21] In our study, we improved the keratin specificity of mutants S180G and E208S by enlarging the width of the S1 pocket.

The position 215 in the center of S1 pocket may be the main residue to decide binding ability of peptides, such as AAPF and AAPL. Tyr215 in KerSMD was corresponding to the conserved Gly166 in subtilisin E or BPN'.[14, 27, 31] There have been many studies on site-directed mutagenesis at Gly166 in subtilisin, and that hydrophobic substitutions at position 166 could change catalytic efficiency towards small hydrophobic peptides.[18, 27, 32] Similar to subtilisin, a suitable substitution at position 215 of KerSMD also could improve the substrate specificity to synthetic tetrapeptide. For example, the mutagenesis Tyr215→Gly obtained the maximum activities to AAPF and AAPL by shortening the side chain and reducing the

electrostatic effect to increase the depth of the S1 pocket (Fig. 5). However, further enhancement of hydrophobicity with Ile or Val resulted in a decrease in enzyme activity. This result is similar to the protein engineering of subtilisin BPN' which showed a negative impact on k_{cat}/K_m upon introducing extremely hydrophobic substitutions at position 166.[18]

Since feather keratins contain plenty of Val, Phe and Leu that may introduce hydrophobic forces and resist common proteases such as trypsin and pepsin, it is assumed that keratinolytic activity may be related to the hydrophobic substrates.[2, 5, 7, 19] The protease BprB, high homology with KerSMD, increased keratinolytic activity by mutating Asp180 (Ser180 in KerSMD) into glycine.[28] In our study, the mutant S180G also showed an increase in keratinolytic activity. Besides, the short side chain at position 208 enlarged the S1 pocket to accept the Phe at P1 site (Fig. 5), which was positive to keratinolytic activity.

Fig.6 showed that hydrogen bonds and electric charge in S1 pocket improved thermophilic characterization and thermostability. The mutants Y215S, and S180G/Y215S enhanced thermostability by increased hydrogen bonds linking to Glu208 (Fig. 6). The Glu (position 208 in KerSMD and BprV, position 156 in subtilisin E and BPN') is always conserved in subtilisin proteases, and it provided electrostatic interactions between substrate and enzyme.[27] So, the substitution of Glu208 decreased its optimal temperature or pH. The semi-hydrophilic and hydroxy Ser215 might enhance its interaction with various substrates through hydrogen bonding (Fig. 6). Except for hydrophobic effect, it seemed that non-covalent

interactions, such as hydrogen bond and weaker electrostatic interaction, were important in deciding the substrate specificity of the S1 pocket, but more evidence should be provided.

4 Conclusions

In this study, we investigated the substrate specificity of keratinase KerSMD by site-directed mutagenesis. Sequence alignment and homologous modeling allowed an insight into the relationship between the S1 pocket and substrate specificity. We found that enlargement of the S1 pocket by mutating residues Ser180, E208, and Y215 improved its catalytic activity to synthetic peptides as well as feather keratin. Reducing steric hindrance at residue 215 was favorable for protease activities on casein and feather. We obtained five mutants (Y215G, Y215S, Y215A, S180G/Y215A, and S180G/Y215S) with improved keratinolytic activities, and two mutants Y215S and S180G/Y215S with improved thermal properties. The results verified that S1 pocket was important to decide substrate specificity and thermostability of keratinase, and selecting short side chain or/and hydrophobic substitution for site-directed mutagenesis probably had positive effect. Our work provided a foundation for future protein engineering to enhance substrate specificity of keratinase.

Acknowledgements

This project was financially supported by the National High Technology Research and Development Program of China (863 Program, 2011AA100905), the Major State

Basic Research Development Program of China (973 Program, 2013CB733902), the National Natural Science Foundation of China (31470160), China Postdoctoral Science Foundation funded projects (114957 and 2013M540538), the Natural Science Foundation of Jiangsu Province (BK2012553), and the 111 Project (111-2-06).

References

1 M. C. Papadopoulos, A. R. El Boushy, A. E. Roodbeen, E. H. Ketelaars, *Anim. Feed Sci. Technol*., 1986, **14**, 279-290.

2 R. Fraser, T. MacRae, G. E. Rogers, in *Keratins: Their Composition, Structure, and Biosynthesis*, ed. Charles C. Thomas, 1972.

3 A. Onifade, N. Al-Sane, A. Al-Musallam, S. Al-Zarban, *Bioresour. Technol*., 1998, **66**, 1-11.

4 R. Gupta, P. Ramnani, *Appl. Microbiol. Biotechnol*., 2006, **70**, 21-33.

5 A. Brandelli, *Food Bioprocess Technol*., 2008, **1**, 105-116.

6 J. Wang, J. Garlich, J. Shih, *J. Appl. Poultry Res*., 2006, **15**, 544-550.

7 A. Brandelli, D. Daroit, A. Riffel, *Appl. Microbiol. Biotechnol*., 2010, **85**, 1735-1750.

8 T. Kornillowicz-Kowalska, J. Bohacz, *Waste Manage*., 2011, **31**, 1689-1701.

9 R. Gupta, R. Rajput, R. Sharma, N. Gupta, *Appl. Microbiol. Biotechnol*., 2013, **97**, 9931-9940.

10 J. Gong, Y. Wang, D. Zhang, R. Zhang, C. Su, H. Li, X. Zhang, Z. Xu, J. Shi, *RSC Adv*., 2015, **5**, 24691.

11 R. Gupta, R. Sharma, Q. K. Beg, *Crit. Rev. Biotechnol*., 2013, **33**, 216-228.

12 D. J. Daroit, A. Brandelli, *Crit. Rev. Biotechnol*., 2014, **34**, 372-384.

13 K. L. Evans, J. Crowder, E.S. Miller, *Can. J. Microbiol*., 2000, **46**, 1004-1011.

14 P. N. Bryan, *Biochim. Biophys. Acta (BBA) - Protein Structure and Molecular Enzymology*, 2000, **1543**, 203-222.

15 E. Di Cera, *Nat. Chem. Biol*., 2008, **4**, 270-271.

16 A. de Kreij, B. van den Burg, O. R. Veltman, G. Vriend, G. Venema, V. G. Eijsink, *Eur. J. Biochem*., 2001, **268**, 4985-4991.

17 H. Takagi, T. Maeda, I. Ohtsu, Y. C. Tsai, S. Nakamori, *FEBS letters*, 1996, **395**, 127-132.

18 D. Estell, T. Graycar, J. Miller, D. Powers, J. Wells, J. Burnier, P. Ng, *Science*, 1986, **233**, 659-663.

19 J. Bradbury, *Adv. Protein Chem*., 1973, **27**, 111-211.

20 Z. Fang, J. Zhang, B. Liu, G. Du, J. Chen, *Int. Biodeterior. Biodegrad*., 2013, **82**, 166-172.

21 Z. Fang, J. Zhang, B. Liu, L. Jiang, G. Du, J. Chen, *Process Biochem*., 2014, **49**, 647-654.

22 B. Liu, J. Zhang, B. Li, X. Liao, G. Du, J. Chen, *World J. Microbiol. Biotechnol*., 2013, **29**, 825-832.

23 S. Windhorst, E. Frank, D.N. Georgieva, N. Genov, F. Buck, P. Borowski, W. Weber, *J. Biol. Chem*., 2002, **277**, 11042-11049.

24 N. Eswar, B. Webb, M. A. Marti-Renom, M. S. Madhusudhan, D. Eramian, M.

Shen, U. Pieper, A. Sali, in *Comparative Protein Structure Modeling Using Modeller, in: Current Protocols in Bioinformatics*, ed. John Wiley & Sons, Inc., 2002.

25 M. Häckel, H. Hinz, G. R. Hedwig, *Biophys. Chem*., 1999, **82**, 35-50.

26 J. Kyte, R. F. Doolittle, *J. Mol. Biol*., 1982, **157**, 105-132.

27 J. A. Wells, D. B. Powers, R. R. Bott, T. P. Graycar, D.A. Estell, *Proc. Natl. Acad. Sci. U. S. A.*,1987, **84**, 1219-1223.

28 W. Wong, L. C. Wijeyewickrema, R. M. Kennan, S. B. Reeve, D. L. Steer, C. Reboul, A. I. Smith, R. N. Pike, J. I. Rood, J. C. Whisstock, *J. Biol. Chem*., 2011, **286**, 42180-42187.

29 D. Georgieva, S. Stoeva, W. Voelter, N. Genov, C. Betzel, *Arch. Biochem. Biophys*., 2001, **387**, 197-201.

30 C. Betzel, S. Klupsch, G. Papendorf, S. Hastrup, S. Branner, K. S. Wilson, *J. Mol. Biol*. 1992, **223**, 427-445.

31 M. Takahashi, Y. Hasuura, S. Nakamori, H. Takagi, *J. Biochem*., 2001, **130**, 99-106.

32 M. D. Ballinger, J. Tom, J. A. Wells, *Biochem*., 1995, **34**, 13312-13319.

33 C. Gao, D. Lan, L. Liu, H. Zhang, B. Yang, Y. Wang, *Biochimie*, 2014, **102**, 29-36.

34 Z. Fang, J. Zhang, B. Liu, G. Du, J. Chen, *Microb. Biotechnol.*, 2015, doi:10.1111/1751-7915.12300.

468 **Table 1** Biochemical properties of the wild type and its mutants.

Mutant	T_{opt} (^oC)	pH_{opt}	Caseinolytic activity (U mg^{-1})	Keratinolytic activity (U mg^{-1})	k_{cat}/K_m (mM s^{-1})			
					AAPF	AAPL	AAPV	AAPA
WT	60	8	3379±68	3409±73	71	33	3.2	25
S180G	55	7	2250±54	3668±70	87	36	3.4	28
E208N	60	7	3290±46	3506±54	84	42	3.8	28
E208S	70	9	2690±68	3612±58	126	46	4.2	22
Y215G	60	8	7200±123	4320±23	365	84	3.4	12
Y215T	65	9	3360±64	3821±36	142	65	3.4	18
Y215Q	55	7	3012±58	1430±122	48	11	1.8	23
R216W	60	8	3420±48	3458±242	74	34	3.2	26
R216Y	60	8	3450±52	3500±48	72	33	3.2	25

469

470

471

472

473

474

475

476

477

478 **Table 2.** Effect of hydrophobicity at position 215 on caseinolytic and keratinolytic
479 activities of different mutants.

Mutant	Hydrophobicity	Caseinolytic activity (U mg^{-1})	Keratinlytic activity (U mg^{-1})
Y215N	-3.5	1760±45	1210±78
Y215P	-1.6	250±80	762±56
WT	-1.3	3379±68	3409±73
Y215W	-0.9	510±105	2630±120
Y215S	-0.8	3890±20	4029±152
Y215T	-0.7	3360±46	3821±45
Y215G	-0.4	7200±85	4320±120
Y215A	1.8	960±28	4120±105
Y215M	1.9	790±24	1350±78
Y215C	2.5	3672±36	1120±30
Y215F	2.8	3290±60	3700±80
Y215L	3.8	1042±25	790±80
Y215V	4.2	1260±45	1104±62
Y215I	4.5	790±28	1220±110

480
481
482
483

484 **Table 3**. The catalytic parameters and protease activities of the wild type and different

485 combinational mutants on tetrapeptide substrate.

Mutant	AAPF		
	K_m (mM^{-1})	k_{cat} (s^{-1})	k_{cat}/K_m ($mM\ s^{-1}$)
WT	0.66±0.04	46.0±0.4	71.0
S180G/Y215G	0.34±0.05	32.0±1.2	94.1
S180G/Y215A	0.30±0.02	45.0±2.0	150.0
S180G/Y215S	0.33±0.02	78±2.4	236.4
S180G/Y215F	0.52±0.10	43±0.5	82.7
E208S/Y215G	0.52±0.12	65±0.8	125.0
E208S/Y215A	0.36±0.02	40±1.2	111.1
E208S/Y215S	0.83±0.02	28±0.8	33.7
E208S/Y215F	0.68±0.08	46±1.8	67.6
S180G/E208S	0.50±0.10	57±2.0	114.0
S180G/E208S/Y215G	0.22±0.01	38±0.8	172.7
S180G/E208S/Y215A	0.41±0.01	67±4.0	163.4
S180G/E208S/Y215S	1.2±0.01	46±2.5	38.3
S180G/E208S/Y215F	0.62±0.02	50±1.8	80.6

486

487

488

Figure captions:

Fig. 1. Homology model of KerSMD (A and B) and alignment of amino acid sequences around the S1 pockets (C). (A) Green residues are the catalytic triad while the predicted S1 pocket is yellow residues and loop. (B) The S1 pocket is showed on the model surface, the nitrogen, oxygen, and carbon atoms are shown in blue, red, and yellow. (C) Sequence alignment of BprV (3TI7), Fervidolysin (1R6V), subtilisin E (1SCJ), subtilisin BPN' (1SBT), and KerA (AAB34259). The amino acids of the S1 pockets are in box. Vertical arrows indicate the mutation sites. Line stands for loops, S for helices, and H for strands.

Fig. 2. Effect of different volume side chains of amino acids at position 215 on catalytic efficiency for the P1 substrates of AAPF, AAPL, and AAPA. The amino acids are written in capital letters. The standard error of k_{cat}/K_m values were all below 5%.

Fig. 3. Specific activities of the wild type and mutants to casein and feather keratin.

Fig. 4. Effect of temperature on the activity (A) and stability at 50 °C (B) of the wild type keratinase and mutants Y215G, Y215S, Y215A, S180G/Y215A, and S180G/Y215S.

Fig. 5. Structure models of keratinase KerSMD mutants, generated with PyMol software. The amino acids of catalytic triad are shown in sticks and the S1 pocket is the colored region. The carbon, nitrogen, and oxygen atoms are shown in yellow, blue, and red, respectively. (A) wild type; (B) Y215A; (C) Y215S; (D) Y215G; (E) S180G/Y215A; (F) S180G/Y215S.

511 **Fig. 6.** Changes in S1 pocket structure and hydrogen bond of wild type, Y215S, and
512 S180G/Y215S. The residues are showed in yellow sticks with red hydroxy. Hydrogen
513 bond is drawn with green dash and the distance is calculated by PyMol software.
514
515
516
517
518
519
520
521
522
523
524
525
526
527
528
529
530
531
532

Fig. 1

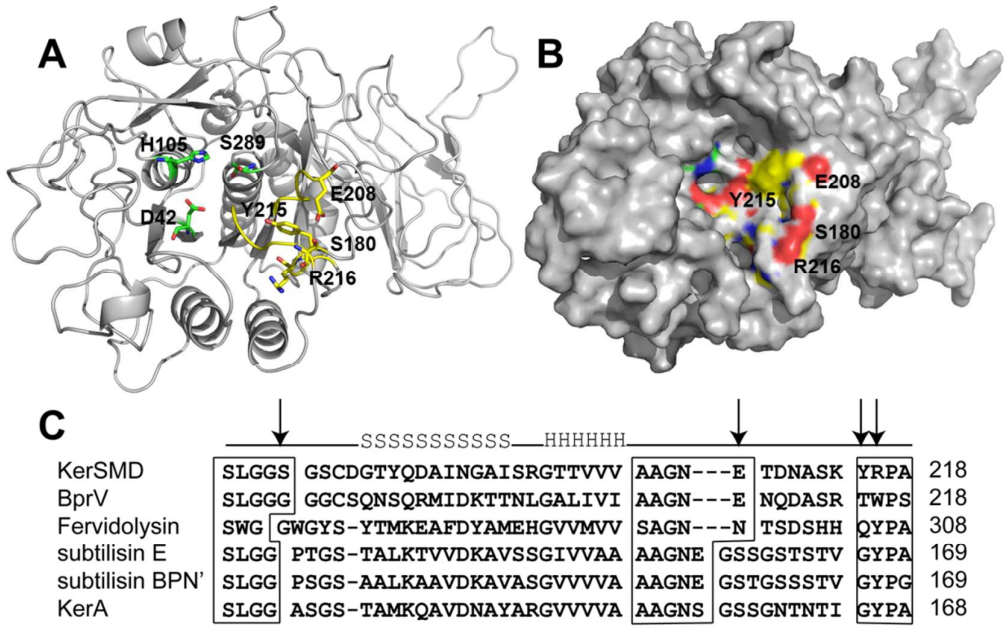

548 Fig. 2

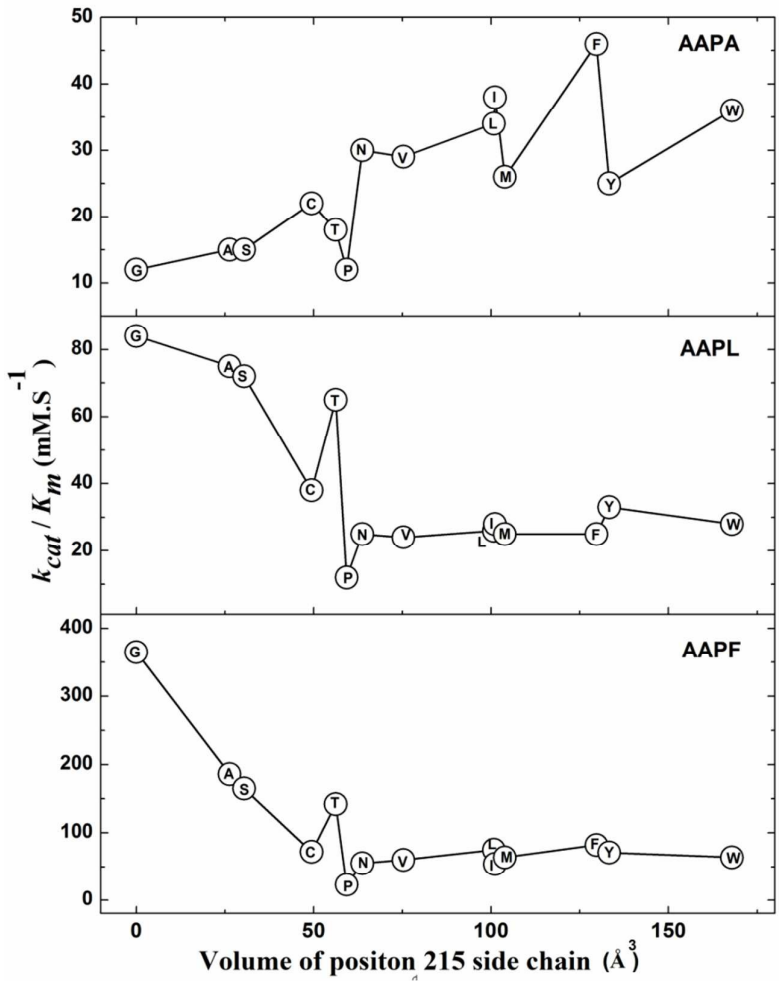

549

550

551

552

553

554

555

556

557

558 Fig. 3

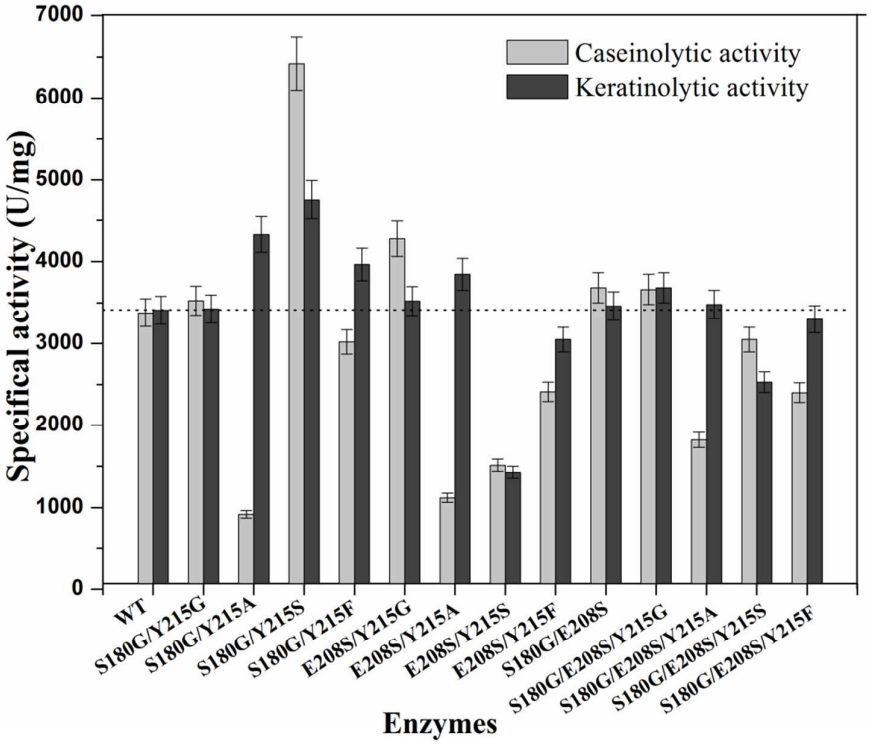

559

560

561

562

563

564

565

566

567

568

569

570

571 Fig. 4

572 A

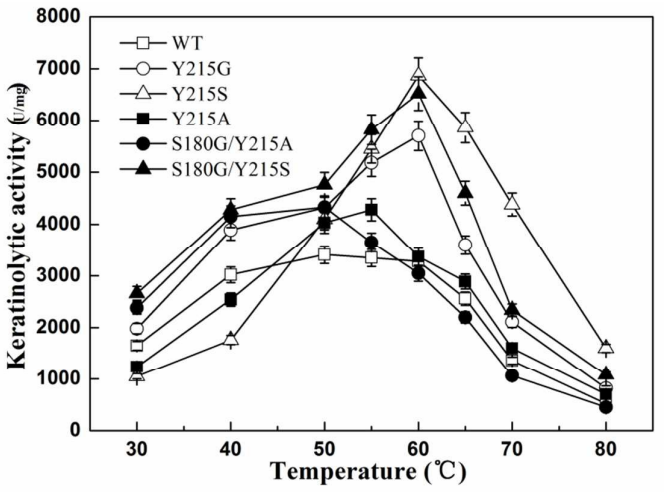

573

574 B

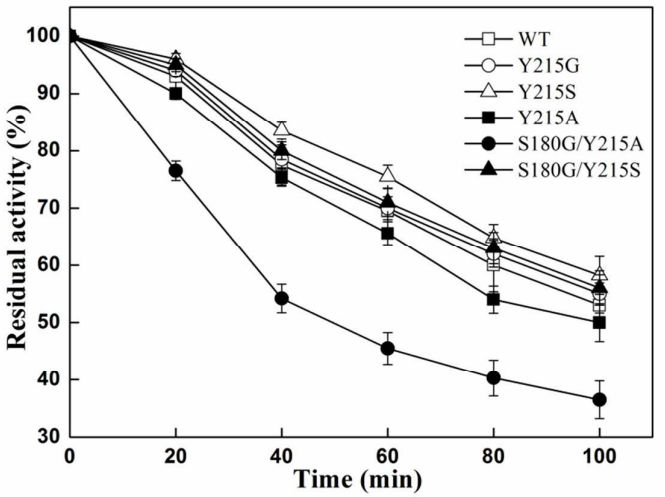

575

576

577

578

579

580

581

582 Fig. 5

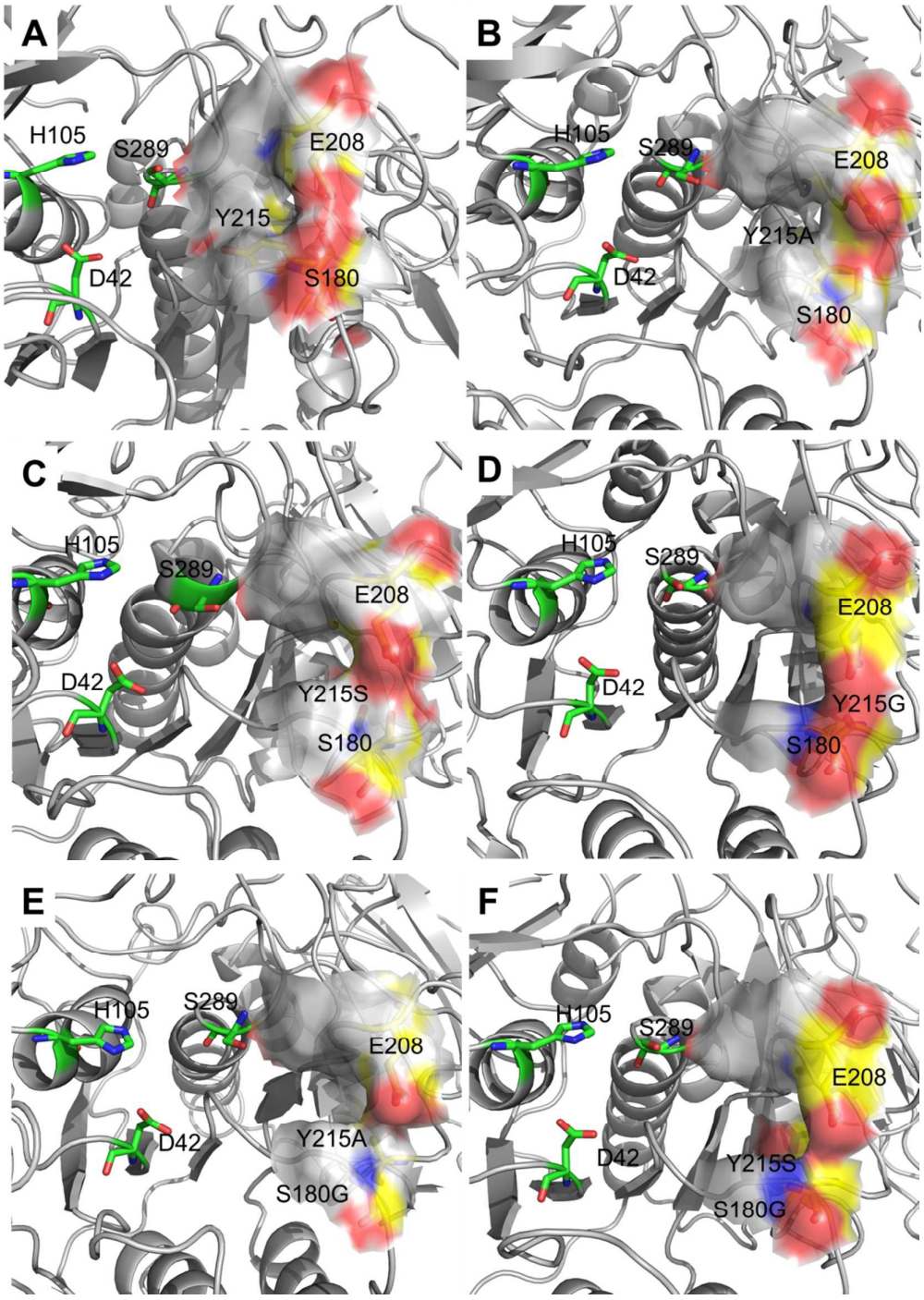

583

584

585

586

587

588

589 Fig. 6

590 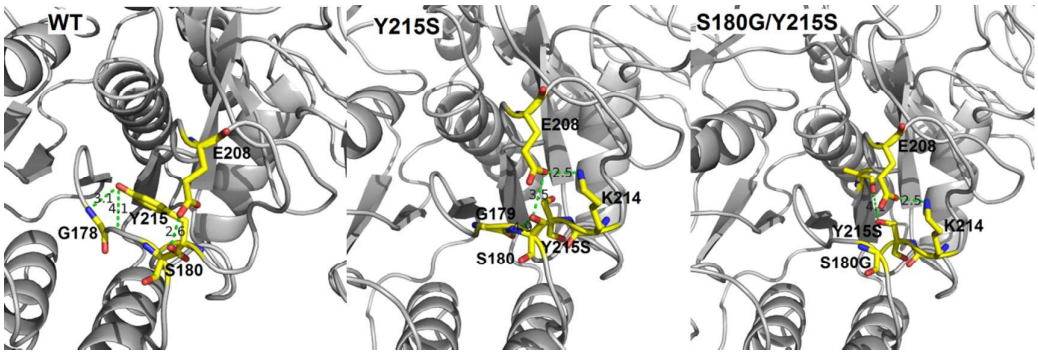

591

592

593

594

595

596